Effect of Start of Injection on the Particulate Emission from Methanol Fuelled HCCI Engine

Article *in* SAE International Journal of Fuels and Lubricants · June 2011

DOI: 10.4271/2011-01-2408

2 authors, including:

Avinash Kumar Agarwal
Indian Institute of Technology Kanpur
582 PUBLICATIONS **23,245** CITATIONS

SAE International

Effect of Start of Injection on the Particulate Emission from Methanol Fuelled HCCI Engine

2011-01-2408
Published
12/15/2011

Rakesh Kumar Maurya
I I T Kanpur

Avinash Kumar Agarwal
I I T Kanpur

doi:10.4271/2011-01-2408

ABSTRACT

New combustion concepts developed in internal combustion engines such as homogeneous charge compression ignition (HCCI) have attracted serious attention due to the possibilities to simultaneously achieve higher efficiency and lower emissions, which will impact the environment positively. The HCCI combustion concept has potential of ultra-low NO_X and particulate matter (PM) emission in comparison to a conventional gasoline or a diesel engine. Environmental Legislation Agencies are becoming increasingly concerned with particulate emissions from engines because the health and environmental effects of particulates emitted are now known and can be measured by sophisticated instruments. Particulate emissions from HCCI engines have been usually considered negligible, and the measurement of mass emission of PM from HCCI combustion systems shows their negligible contribution to PM mass. However some recent studies suggest that PM emissions from HCCI engines cannot be neglected.

In this paper, effect of start of injection (SOI) of fuel on particulate emission of a HCCI engine fuelled with methanol is experimentally investigated. In this study, port fuel injection technique is used for preparing homogeneous mixture of methanol and air. The experiment is conducted with varying SOI timings for different amount of fuel, and intake air temperature. The engine exhaust particle sizer (EEPS) is used for size, surface area and volume distributions of soot particles emitted under each of these different operating conditions. It was found that total concentration of particles increase with increasing intake air temperature and particles are mainly in the size range from 10 to 150 nm. It was found that number and size distribution of HCCI generated soot particles depends on SOI, amount of fuel injected and the intake air temperature.

INTRODUCTION

New emission legislation and standards concerning environmental protection demand further improvements in internal combustion (IC) engine performance, emissions and fuel consumption. Researchers working in the area of IC engines for automotive applications have developed various technologies including catalysts and intelligent engine management systems that have contributed to the achievement of lower emissions and fuel consumption. Furthermore few alternative combustion technologies are also being investigated, HCCI combustion being one of the major candidates. HCCI combustion concept shows potential to reduce fuel consumption and NO_x emissions that meets the most stringent legislations of today and also the future. The earliest reported work [1-2] showed the basic characteristics of HCCI, which have been validated by subsequent researchers, namely: very little cyclic variations and no flame propagation. The HCCI combustion process has been studied with reasonable success in two stroke engines [1-2] and four stroke engines [3,4,5], and with liquid [1,2,3,4,5] and gaseous [6-7] fuels. Due to the economics of large scale production of the alcohol fuels, only methanol and ethanol are suitable as standalone alternative fuels. Both methanol and ethanol exhibit good combustion characteristics in HCCI mode. In particular, methanol has demonstrated a significant widening of the HCCI operating regime compared to gasoline [8]. Although higher carbon monoxide (CO) and hydrocarbon (HC) emissions are usually reported for HCCI combustion

engines, their levels may vary between engines. Particulate emissions from HCCI engines have been usually considered negligible, and the measurement of particulate matter (PM) with HCCI combustion systems is reported very scarcely. There is very little information available in open literature regarding the particulate matter emission from the HCCI combustion engine.

Emissions of PM, especially small sized particles emitted from engines have great impact on urban air quality and human health. Correlation between human health and level of PM is shown by researchers [9]. Particle size influences the environmental impact in several ways e.g. it influences residence time of the particulate in the atmosphere, optical properties of the particulate, particle surface area, its ability to participate in atmospheric chemistry, and its health impacts. The optical properties of PM influence atmospheric visibility and are responsible for soiling of buildings. These properties depend on particle size, shape, and composition [10]. Particles interact with light by absorbing/ scattering it. For diesel exhaust particulate, absorption is much stronger than scattering and is relatively independent of particle size for visible light. The absorption is primarily due to the carbon content of the particulate. Light scattering is strongly dependent on particulate size and shape and is typically maximum for particulate a few tenths of a micron in diameter. The scattering is mainly due to particles in the accumulation mode size range. Ultrafine particles (Dp<100 nm) and nano-particles scatter light very weakly. Most of the particle numbers emitted by internal combustion engines lie in the nano-particle range (<50 nm), while most of the particulate mass lies in the accumulation mode size range (50 nm < D < 1000 nm) [11].

With HCCI combustion, emissions of PM, or smoke, are frequently described as “near zero” or “ultra-low” [12]. However recent investigations have shown that although the total mass of PM is indeed low, significant numbers of particles remain in the size ranges below 100 nm mobility diameter [13,14,15,16,17]. This size range is well within the measurement capabilities of modern nano-particle instrumentation, which is well suited for studies in HCCI particle emissions. Kaiser et al. investigated PM emissions from gasoline fueled HCCI engine, which uses an early direct injection strategy at various fuel injection timings [13]. A scanning mobility particle sizer (SMPS) was used for PM measurements in this study. HCCI combustion was achieved with intake temperatures ranging from 150- 200°C at a compression ratio of 15.2:1 and λ ranging from 2 to ≅ 18. Particle size distributions are presented for three different HCCI operating conditions (λ=2.35, 3.25, and 6.77) at a constant engine speed (1100 rpm). In addition, particle size distributions from the same engine running in a DISI mode (λ=1) and motored mode are also shown. At two of the HCCI conditions (λ=2.35 and λ = 3.25), accumulation mode number concentrations were higher than that of DISI operation and the mode itself was found at a larger mobility diameter. The presence of the large accumulation modes was explained by the existence of at least some degree of diffusion burning. Price et al. reported PM emissions from a gasoline fueled HCCI engine using DI-HCCI fueling strategy and a multiple electrometer based differential mobility particle sizer [14]. Tests were conducted by varying valve timings and intake air temperatures. All tested conditions with different valve timing combinations showed a nucleation mode that had a significantly higher particle concentration than the accumulation mode. Misztal et al. conducted more detailed study of HCCI particle size distributions using DI-HCCI system by injecting unleaded gasoline directly into the cylinder employing negative valve overlap (NVO) to capture residuals [15]. Other investigation by Misztal et al. examined the role of injection timing in PM formation in the same engine [16]. The DI mode of fuel delivery led to discovery of high sensitivity of PM formation to injection timings. Injection timings were reported in terms of end of injection (EOI) and were varied from 250° BTDC to 350° BTDC of the compression stroke. The most advanced timings generally showed the highest PM mass and number emissions even though mixing times were the longest. The authors attributed this to wall wetting effects from impingement of most of the fuel on the piston surfaces. They also noticed that PM emissions were very closely coupled to mixture homogeneity for this type of HCCI engine.

Many HCCI combustion studies use port fuel injection techniques for homogenous charge preparation [3,4,5, 17,18,19]. Herold et al. investigated the effect of port fuel injection timing on the combustion and emission characteristics of HCCI combustion engine but particulate emissions were not reported [19]. Recent studies investigated effect of port injection timing on exhaust emission excluding PM emissions in spark ignition engine [20-21]. All facts mentioned above lead to the conclusion that the thermal conditions and injection timing, at which HCCI engine is operated will affect emissions, including PM emissions. Particulate emission data for port fuel injected HCCI combustion is not available in open literature therefore it is worth investigating the effect of fuel injection timings and inlet air temperature on PM emissions from HCCI engines.

EXPERIMENTAL SETUP

A four-cylinder, four-stroke, water-cooled, naturally-aspirated, direct-injection diesel engine (Make: Mahindra and Mahindra, India; Model: Loadking NEF 3200 TCI) was modified for the experiments. The specifications of the unmodified test engine are given in table 1. The engine was coupled with an eddy current dynamometer (Make: Dynalec (Pune), India; Model: ECB 200). One of the four cylinders of the engine was modified to operate in HCCI mode, while the other cylinders operate like an ordinary diesel engine, thus motoring the first cylinder for attaining HCCI combustion.

The intake and exhaust manifold of HCCI combustion cylinder were separated from the other three CI cylinders. Schematic diagram of the experimental setup is shown in figure 1. Test fuel used for the present investigation is methanol. The fuel was premixed with air through port fuel injector installed in the intake manifold of the HCCI cylinder. Electronic fuel injector (4 nozzle holes) injected the fuel in the engine manifold at 3 bars fuel injection pressure. The fuel pressure of 3 bars was developed by the fuel pump installed in the gasoline tank. The quantity of fuel and injection timing was controlled by a micro-processor (Make: National Instruments, Model: Compact-RIO 9014) through a customised driver circuit. Compact-RIO microprocessor (Reconfigurable Input-Output) combined an embedded real-time processor, a high-performance field-programmable gate array (FPGA), and hot-swappable input/ output (I/O) modules. Each I/O module was connected directly to the FPGA, providing low-level customization of timing and I/O signal processing. The FPGA was connected to the embedded real-time processor via a high-speed PCI bus. Compact-RIO was programmed by LabVIEW FPGA and LabVIEW Real-Time module softwares. LabVIEW contained built-in data transfer mechanisms to pass data from the FPGA to the embedded real-time processor for online data analysis, data logging, or communication to a networked host computer. The Compact-RIO acquired signals from a high precision rotary shaft encoder (Make: BEI, USA; Model: H25D-SS-2160-ABZC), Air mass meter (Make: Bosch, Germany; Model: HFM5) and an in-cylinder piezo-electric pressure sensor (Make: Kistler, Switzerland; Model: 6013C). Compact-RIO generated the output pulse to operate the fuel injector based on the analysis of the acquired signals and engine operating conditions. Based on the output pulses generated by Compact-RIO, fuel injector injected the required amount of fuel in to the intake manifold.

Table 1. Test engine specifications.

Make	M&M Ltd., India
Model	Load King NEF 3200 TCI
Displaced volume	2609 cc
Stroke/ Bore/ No. of cylinders	94 mm/ 94 mm/ 4
Connecting Rod Length	158 mm
Max Engine Output	53.5 kw (72.7 HP) @ 3200 rpm
Max Torque	195 Nm @ 1900 – 2000 rpm
Number of Valves/ Cylinder	2

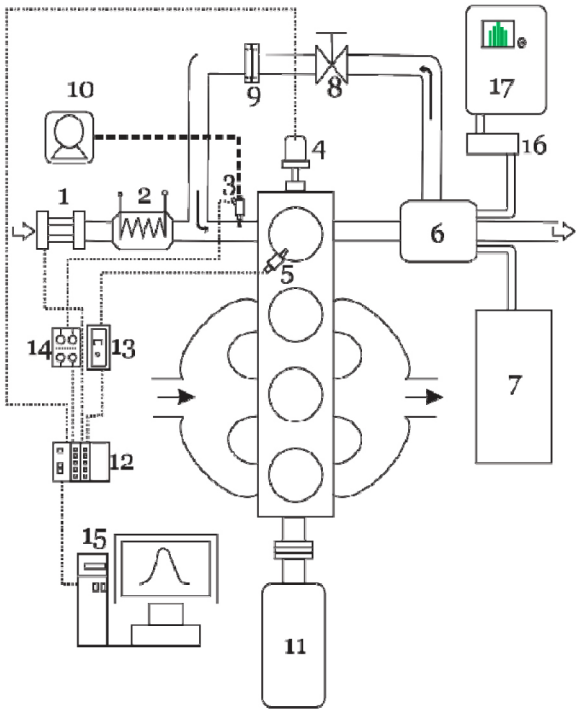

1. Hot-film Air Mass Meter 2. Air Heater 3. Fuel Injector
4. Rotary Shaft Encoder 5. Pressure Transducer
6. Exhaust Plenum 7. Emission Analyzer 8. EGR Valve
9. Orifice 10. Fuel Tank with Pump 11. Dynamometer
12. Compact RIO 13. Charge Amplifier 14. Driver Circuit
15. Computer 16. Exhaust Gas Diluter 17. EEPS

Figure 1. Schematic diagram of the experimental setup.

Actual air mass delivered to HCCI combustion cylinder was measured by hot-film air mass meter accurately. To achieve HCCI combustion, the air-fuel mixture was preheated to a suitably high temperature prior to intake stroke of the cylinder. For this, fresh air entering the engine was heated by an air pre-heater positioned upstream of the intake manifold. The intake air heater was operated by a closed loop temperature controller, which maintained constant intake air temperature as set by the user. The heater controller takes feedback from a thermocouple installed in the intake manifold immediately upstream of the fuel injector. Thermocouples with a multi-channel digital temperature indicator were used for measuring the intake and exhaust gas temperatures. Provision for exhaust gas recirculation (EGR) was made so that some of the exhaust gas can also be re-circulated in intake manifold through EGR valve for controlling the combustion timing and duration. The in-cylinder pressure was measured using a piezoelectric pressure transducer mounted flush with the cylinder head. To measure the crank angle position, a high precision optical shaft encoder was coupled with the crankshaft using a helical coupling. The in-cylinder pressure history data acquisition and combustion analysis was done using a LabVIEW based program, which was developed at the Engine Research

Laboratory, IIT Kanpur. In-cylinder pressure of the HCCI cylinder was recorded for 2000 consecutive engine cycles for each engine operating conditions with 1/6th CAD resolutions and analyzed to calculate the detailed combustion phasing parameters.

PARTICULATE SIZE MEASUREMENT

In this study, Engine Exhaust Particle Sizer (EEPS) was used to measure the particulate size and number distribution in the engine exhaust. EEPS is an advanced version of scanning mobility particle size (SMPS) system, which is widely used to measure the size distribution of atmospheric aerosols.The EEPS spectrometer is a fast-response, high-resolution instrument that measures particle number concentrations in diluted engine exhaust. The instrument draws a sample of the exhaust flow into the inlet continuously (Figure 2).

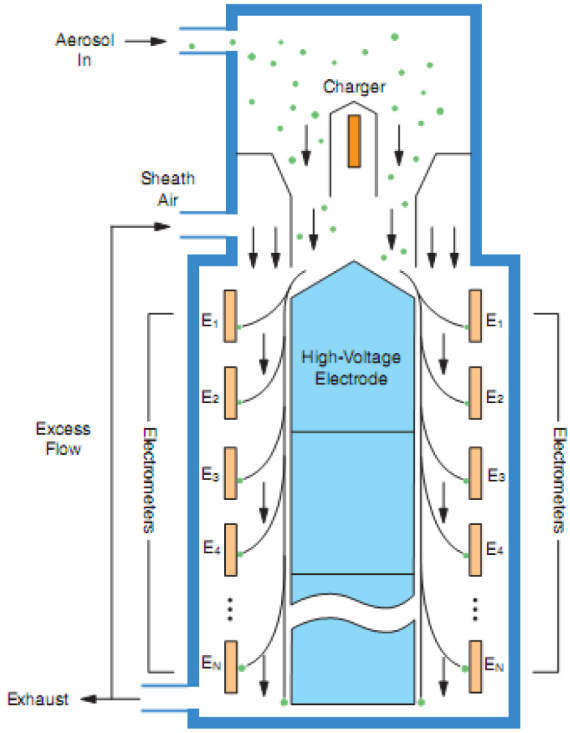

Figure 2. Schematic of EEPS spectrometer.

Particles are positively charged to a predictable level using a corona charger. Charged particles are then introduced to the measurement region near the center of a high-voltage electrode column and transported down the column surrounded by filtered sheath air. A positive voltage is applied to the electrode which creates an electric field that repels the positively charged particles outward according to their electrical mobility. Charged particles strike the respective electrometers and transfer their charge. A particle with higher electrical mobility strikes an electrometer near the top; whereas, a particle with lower electrical mobility strikes an electrometer lower in the stack. This multiple detector arrangement using highly sensitive electrometers allows for simultaneous concentration measurements of multiple particle sizes.

EEPS spectrometer provides both high temporal resolution and reasonable size resolution by using the same basic technique as that of SMPS system but with multiple detectors working in parallel. This makes the EEPS ideal for measuring engine operating under transient conditions. The EEPS is designed specifically to measure particulate emitted from engines and vehicles. It measures particle size from 5.6 to 560 nm with a size resolution of 16 channels per decade (a total of 32 channels). Reading the particle size distribution 10 times per second (10Hz) allows transient measurement possible during an engine measurement. The electrometers are read at 10 Hz frequency by a microprocessor, which then inverts the current/ charge data to particle size and number distribution.

RESULTS AND DISCUSSION

In this section, the experimental results of HCCI combustion particulate emissions for different engine operating conditions at constant speed (1500 rpm) are presented using methanol as fuel. Experiments were conducted for different amount of fueling (21, 25 and 29 mg/stroke) by varying start of injection (SOI) timing at various inlet air temperatures (T_i) of 150, 160, 170 and 180°C respectively. The corresponding relative air fuel ratios (λ) for different fuelling amounts (21, 25 and 29 mg/stroke) are $\lambda = 3.67$, 3.07 and 2.65 respectively. The measurement of particulate size distribution was done after the engine was thermal stabilized at each test condition. The sampling was done for one minute and the sampling frequency was kept at 1 Hz, therefore all results presented in this paper are average of sixty data points collected. Each measurement was repeated twice to ensure the repeatability of trends. The results are presented in the form of number and size distribution in the exhaust stream per unit volume of exhaust (after accounting for the dilution factor). The dilution ratio used by the sampling system (diluter) is 114:1. To investigate the effect of port fuel injection timing on the particulate emissions from the engine, different start of injection timings (5, 70, 210, 500 and 600 CAD) are selected in open and closed intake valve conditions as shown in figure 3. Duration of fuel injection for different amount of fueling is also indicated in the figure by different lengths. The different injection timings affect fuel mixing differently and various degree of fuel unmixedness caused by different injection timings [19]. During closed intake valve fuel injection, majority of fuel spray strikes the base of the intake passage and intake valves. Fuel injection timing has a significant influence on the mixture formation and it depends on several factors such as characteristics of fuel spray in the intake manifold, homogeneity of the mixture at the time of ignition, cold and hot engine operation etc. Details regarding the mixture preparation during closed and open valve injection

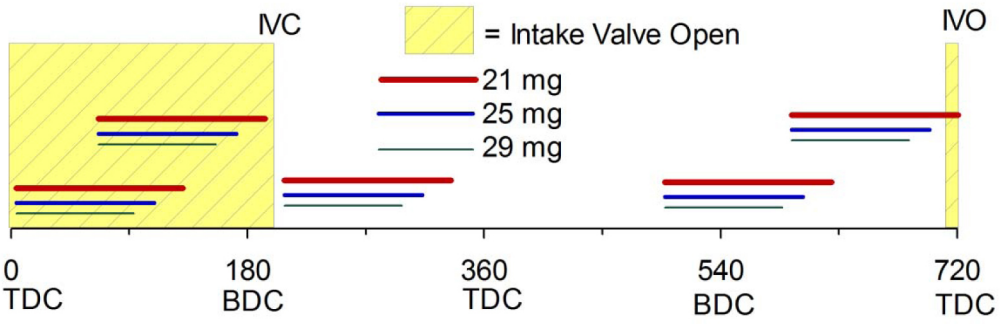

Figure 3. Crank angle injection timings used in port fuel injection experiments (IVC, intake valve closed; IVO, intake valve open).

timing and flow of fuel air mixture with its effect on HC emissions are discussed in detail in 'Gasoline engine management' [22]. The degree of fuel mixing caused by different injection timings is discussed by Harold et al. [19].

Figure 4 shows indicated mean effective pressure (IMEP) variations at different amount of fuel introduced and inlet air temperature by varying the SOI for each test condition. IMEP is an important indication of the usable power per cycle produced by the engine and calculated from measured cylinder pressure. It can be noticed from figure 4a that IMEP is decreasing as engine operates on lesser fuel quantity. It can also be observed from the figure that IMEP was lower for the SOI corresponding to open intake valve. Shaded regions show the open valve duration. Figure 4b shows that upon increasing the intake air temperature, the IMEP decrease for each test condition due to advancing of ignition timings. Maximum IMEP in this investigation was 3.8 bar for 29 mg fueling at intake air temperature of 150 °C.

Figure 5 shows CA50 (crank angle position corresponding to 50% mass burn fraction) position variations as a function of SOI timings for different amounts of fuel introduced and varying inlet air temperature. Crank angle position of CA50 is regarded as combustion phasing in HCCI combustion studies and is a good feedback alternative in order to control HCCI combustion [23]. It can be noticed from figure 5a that on increasing the amount of fuel introduced in the combustion chamber, the combustion phasing advances because richer fuel-air mixture auto-ignites rather easily [24]. At constant fueling, combustion timing advances with increase in intake air temperature (figure 5b). Combustion phasing depends on the air-fuel ratio and inlet air temperature both and more detailed explanation of combustion phasing dependency on different parameters is explained by Dec et al. [24]. For constant fueling and intake air temperature, the combustion phasing depends on the fuel injection timing. It is observed from the figure 5 that for closed valve timing, combustion phasing is earlier as compared to open valve injection due to greater homogeneity of mixture formation during closed valve injection timing and more time available for mixing of fuel and air.

Figure 6 shows maximum rate of pressure rise variation as function of SOI timings for different amount of fuel introduced and inlet air temperatures. Rate of pressure rise affects combustion noise. When the fuelling rates increase (i.e. lower λ), the HCCI combustion rates also increase and intensify, and gradually cause unacceptable noise and can potentially cause engine damage and unacceptably high level of NO_x emissions. Therefore knocking combustion is often used to define the upper limit of HCCI [18]. It can be seen from figures 6a that maximum rate of pressure rise is high for richer fuel-air mixtures and is rather low for leaner fuel-air mixtures. Rate of combustion is a critical parameter to control the HCCI combustion and richer mixtures have very high combustion rates. It can also be noticed from the figure that maximum rate of pressure rise is also dependent on the SOI timings. Closed valve injection timings lead to higher maximum rate of pressure rise for advanced combustion phasing (figure 5a). It is observed from figure 6b that on increasing the intake air temperature, the maximum rate of pressure rise increases due to advanced combustion phasing (figure 5b).

Figure 7a shows the NOx emission as a function of fuel injection timing for different amount of fuel injected per stroke at Ti=150 °C. It can be observed that for all these tests, NOx emissions are limited to 22 ppm, which is very low as compared to conventional combustion engines. For higher amount of fueling, the NOx emissions are higher due to advanced combustion timings (figure 5a). Figure 7b shows HC emissions as a function of the fuel injection timing for different amount of fuel injected per stroke. It can be observed from the figure that for closed valve injection, total unburned HC emissions are almost constant and independent of the fuel injection timings. The HC emissions however increase with open valve injection timings. These observations are consistent with other studies on spark ignition engine [20, 25]. The possible explanation of these observations is that for closed valve injection, most of the

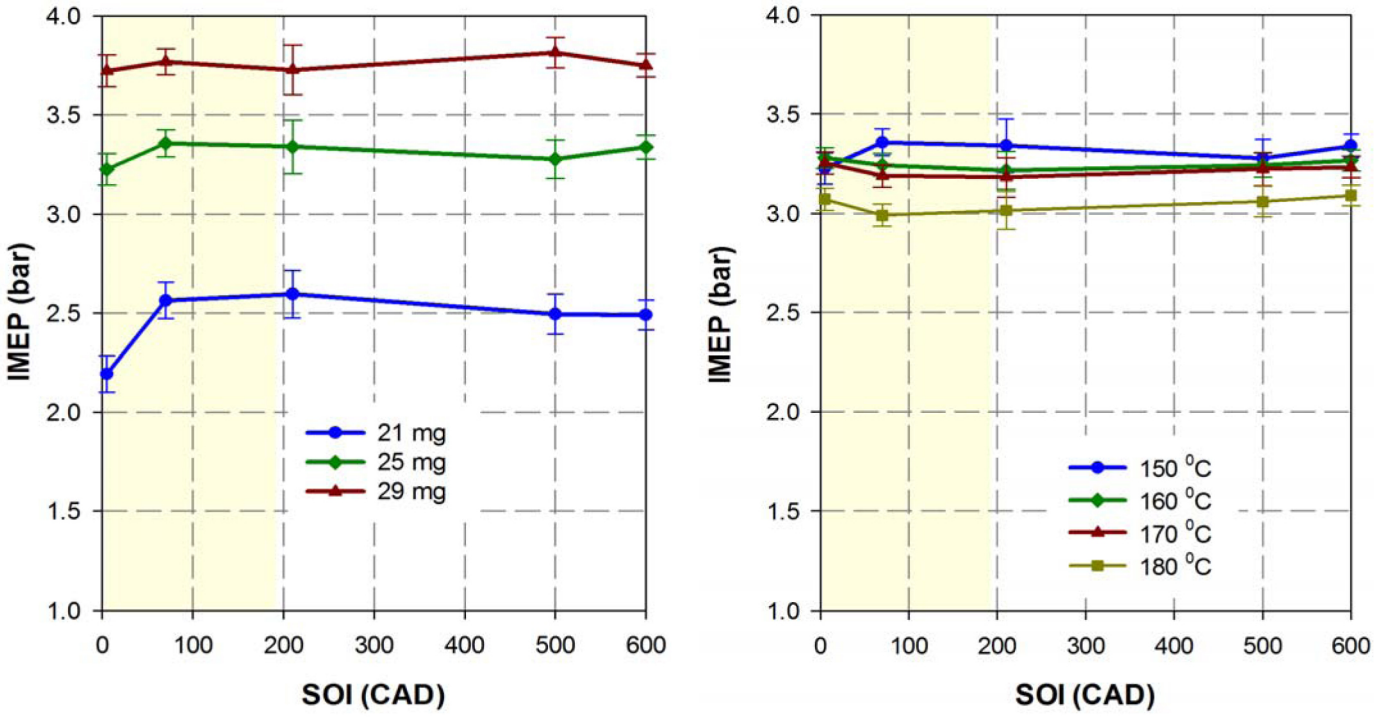

a.for different amount of fuel injected per stroke at T_i=150 ^{0}C b. for different T_i at constant fueling (25mg/stroke)

Figure 4. IMEP variation at 1500 rpm for varying SOI timings.

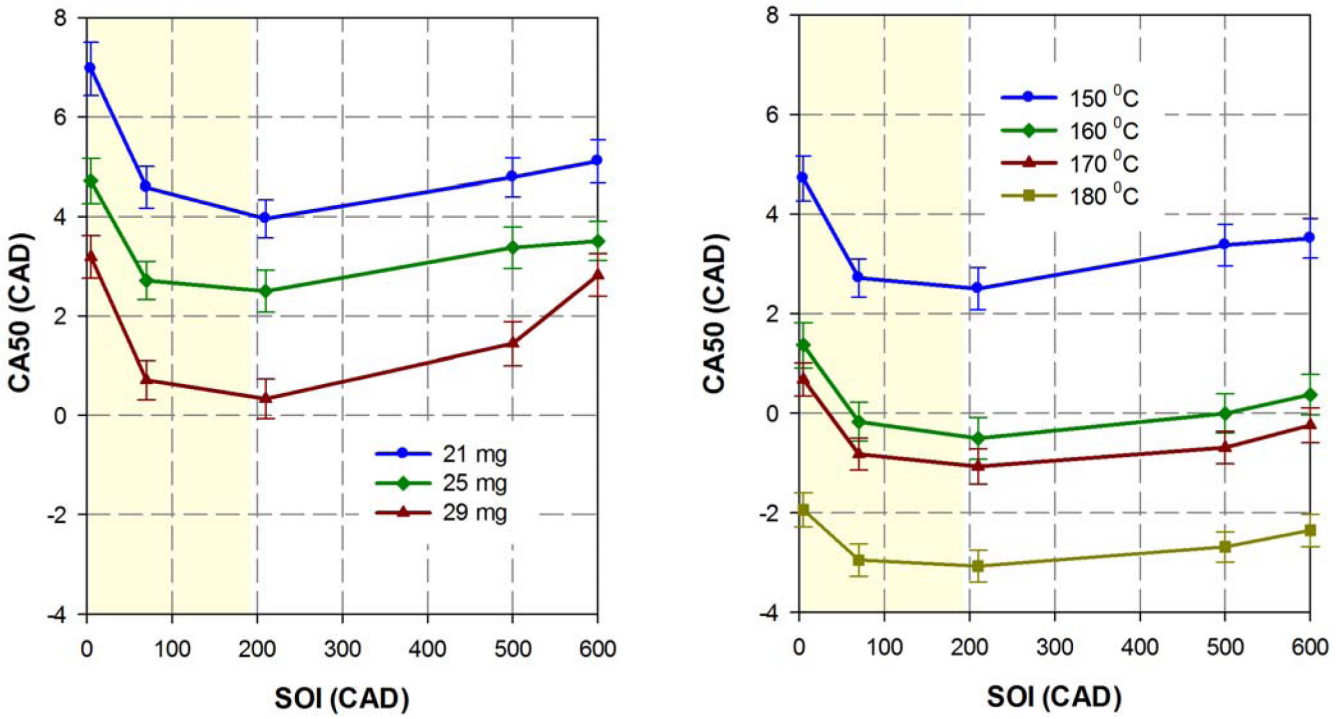

a.for different amount of fuel injected per stroke at T_i=150 ^{0}C b. for different T_i at constant fueling (25mg/stroke)

Figure 5. CA50 variation at 1500 rpm for varying SOI timings.

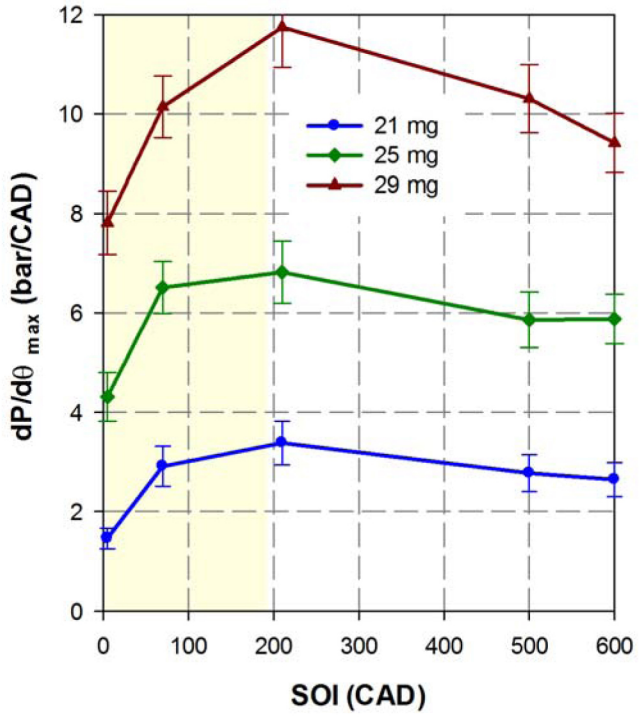

a.for different amount of fuel injected per stroke at T_i=150 ^{0}C

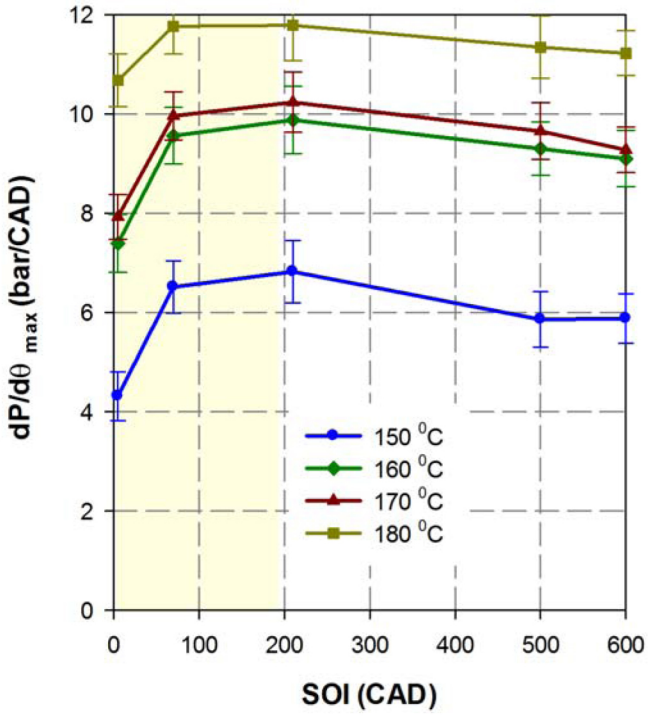

b. for different T_i at constant fueling (25mg/stroke)

Figure 6. Maximum rate of pressure rise variation at 1500 rpm for varying SOI timings.

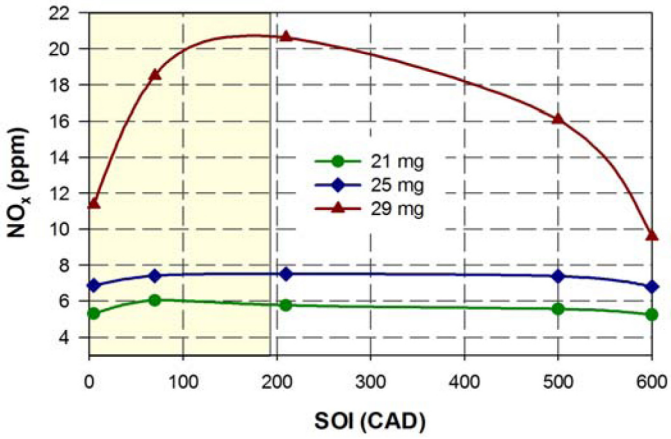

a.NO_x emission for different amount of fuel injected per stroke at T_i=150 ^{0}C

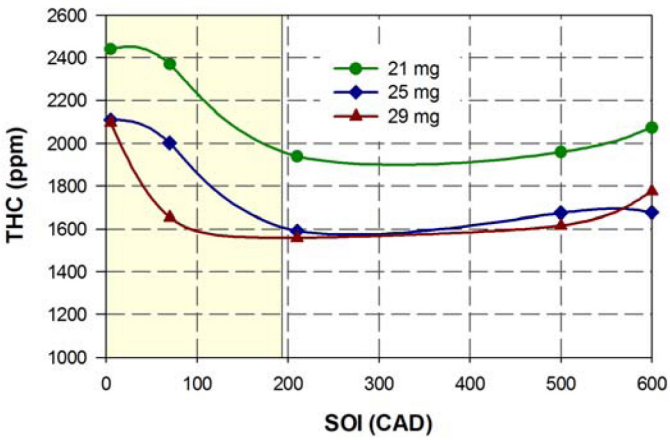

b. HC emission for different amount of fuel injected per stroke at T_i=150 ^{0}C

Figure 7. NOx and HC emission variation at 1500 rpm for varying SOI timings.

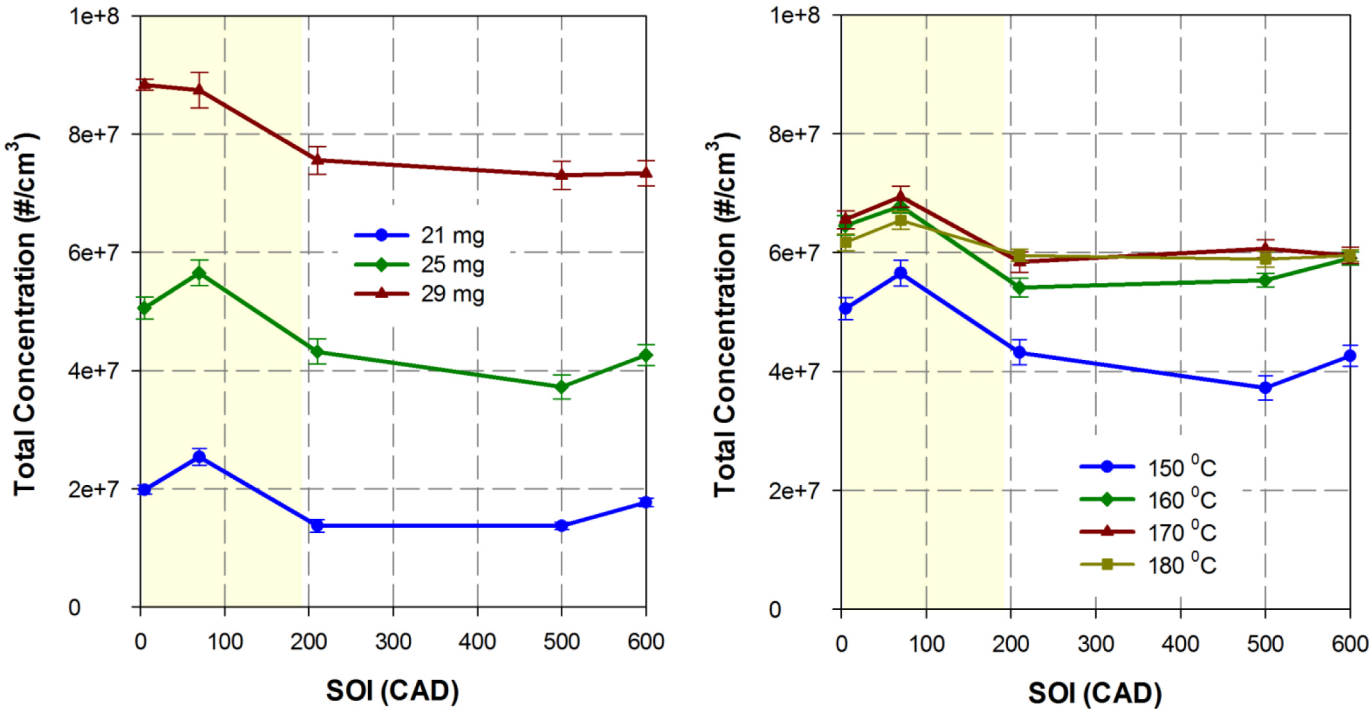

a. for different amount of fuel injected per stroke at T_i=150 ^{0}C

b. for different T_i at constant fueling (25mg/stroke)

Figure 8. Total concentration of particles at 1500 rpm for varying SOI timings.

fuel lands on the port walls before entering the cylinder hence injection details do not really matter much. However for open valve injection, the HC emission increase because more liquid fuel droplets enters the cylinder. These results suggest that closed valve fuel injection will be more suitable for the HCCI engines having PFI system.

Figure 8 shows total number concentration of particles at different amount of fuel/ stroke and T_i by varying the SOI timing for each test condition. It is observed from the figure 8a that total number concentration of particles increase with increasing fuel/stroke in combustion chamber at constant inlet air temperature of 150°C. This suggests that on increasing the fueling (load), total particle concentration increases and trend agrees with observations for engines using conventional combustion modes [15, 26]. The total concentration of particles is higher at richer mixture conditions and comparable for leaner conditions as compared to gasoline HCCI study reported [16]. It can also be noticed that total particle number concentration increases as injection timing get closer towards intake valve open (IVO) injection and concentration is highest for IVO injection for all conditions. The fuel injection timing in intake valve closed (IVC) condition created more homogeneous fuel distribution as compared to IVO injection [19]. This suggests that particulate matter emissions are sensitive to mixture homogeneity. The more homogeneous a mixture is, lesser PM will be emitted [16]. This explains why there is higher concentration of particles during IVO injection timing compared to IVC injection timings.

Figure 8b shows the effect of intake air temperature on the total concentration of particles for constant (25 mg/stroke) fuel injection quantity. It is observed that total concentration of particles increases with increasing intake air temperature up to 170°C and further increasing intake temperature does not increase the total concentration of particles. It can also be noticed that total concentration is higher for IVO injection timings for all intake air temperature conditions as compared to IVC injection timings. It can be further observed that injection timings between 210 - 500 CAD do not show significant variations in the total concentration of particles for most of the test conditions.

NUMBER AND SIZE DISTRIBUTION OF EXHAUST PARTICULATES

Methanol HCCI combustion generated exhaust particle's number and size distribution is depicted in the graph at different SOI at constant engine speed for different quantities of fuel burnt (figure 9) and at different intake air temperature at constant fueling (figure 10). It can be observed (figure 9) that peak concentration of particles increases with increase in fuel quantity/stroke. For each fueling condition, SOI in IVO conditions (5 and 70 CAD) have higher peak particle

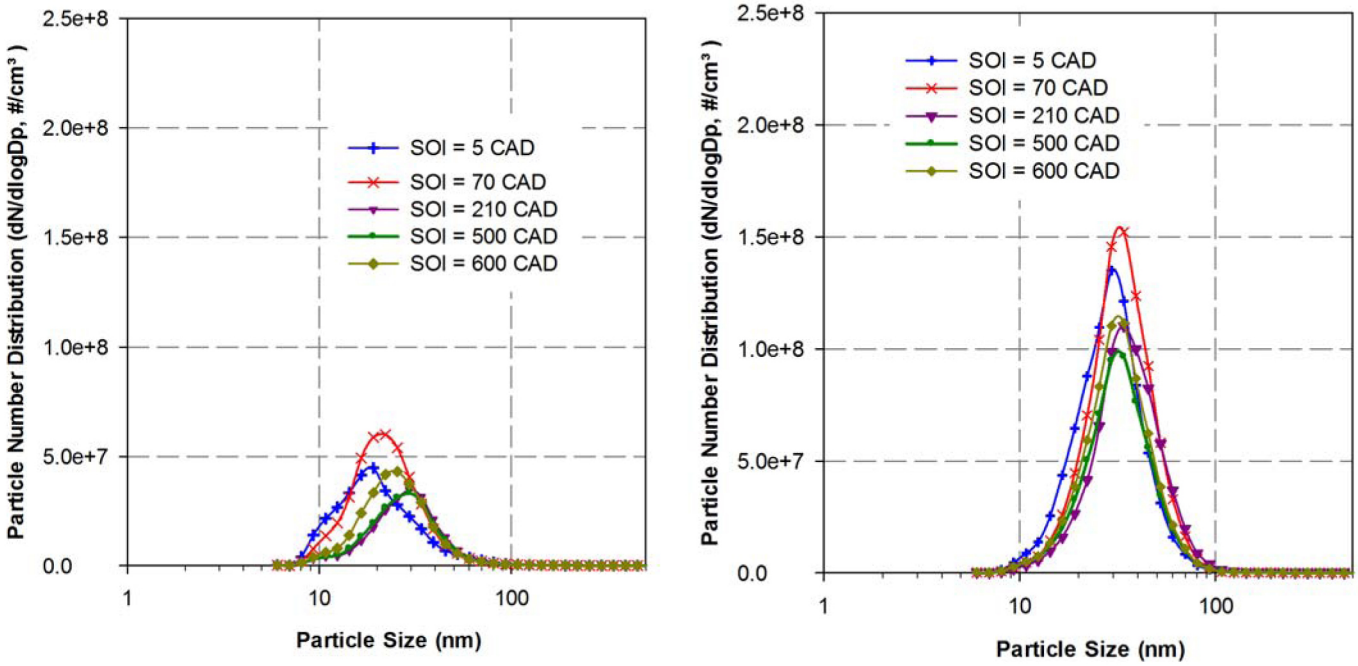

a. 21 mg/stroke fuel

b. 25 mg/stroke fuel

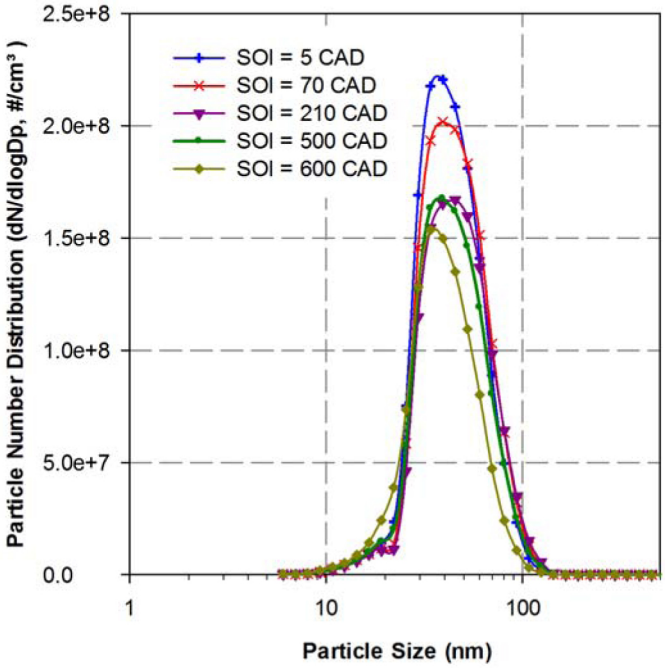

c. 29 mg/stroke fuel

Figure 9. Particle size and number distribution at 1500 rpm for varying SOI for different fuel injection quantities.

concentration as compared to SOI in IVC conditions due to higher mixture homogeneity in IVC timings. It suggests that fuel injection should be done in IVC conditions from particulate emission point of view in port fuel injected HCCI combustion engine. Figure 9 suggests that on increasing the fuel quantity, the particle concentration peak shifts towards higher mobility diameters. For low fueling (21 mg/stroke), peak particle concentrations appear around 20 nm with concentration 6.02×10^7particles/cm^{3}and for higher fueling (25 and 29 mg/stroke), peak particle concentration appears around particle size 32 and 37 nm with concentrations of

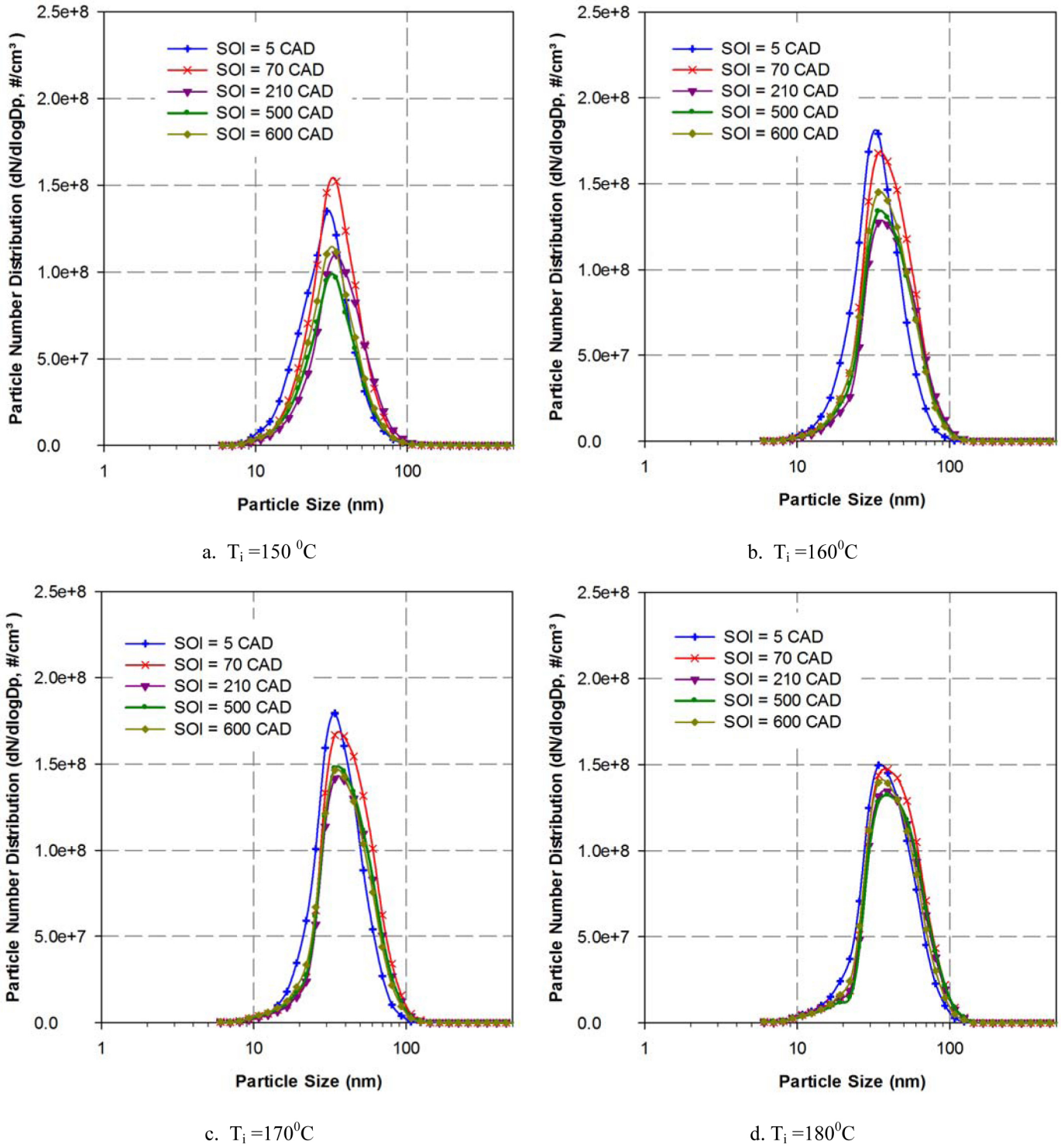

a. T_i =150 ^{0}C

b. T_i =160^{0}C

c. T_i =170^{0}C

d. T_i =180^{0}C

Figure 10. Particle size and number distribution at 1500 rpm with varying SOI for different inlet air temperature.

1.54× 10^8 and 2.23× 10^8particles/cm^3 respectively. The particle size around which peak number concentration of particles is measured is less than 40 nm for all test conditions. Mobility diameters with peak concentration are little higher as compared to gasoline spark ignition (<25nm) [26]. The peak concentrations measured are comparable to those presented for gasoline HCCI combustion [15]. It can also be observed from figure 9 that the distribution width of particulate size increases with increasing fuel quantity. For all the test conditions, the particle sizes having significant

number of particles are in the range of 10- 150 nm. These results are consistent with the data of particulate using ethanol, where the diameter of particles is reported to be smaller than 100 nm [27]. For diameters >~50 nm, the particulate emissions are characteristic of soot particles (possibly coated with condensed hydrocarbons), which are typical of the majority of the mass emissions from diesel and DISI engines. For diameters <~50 nm, the particles are likely to be nucleation mode particles composed of unburned HCs emitted from the exhaust valve [13]. For low fueling (21mg), particles are mainly < 50 nm and as fueling increases, the particles having size >50 nm increases, which means particles are shifted in to soot mode. Smaller particles are more likely to be liquid nucleation particles whereas larger particles are more likely to be solid particles agglomerates.

Figure 10 shows the variation of particle concentrations with SOI timings at different intake air temperatures for constant fuel quantity (25 mg/stroke). It can be observed that for each intake air condition, SOI in IVO conditions (5 and 70 CAD) have higher peak particle concentration as compared to SOI in IVC conditions. Also, the difference between peak concentrations in SOI at IVO open and IVC is lower at higher intake air temperature. It can be noticed that peak concentration of particles increases with increase in intake air temperature up to 170 °C and further increasing intake air temperature does not increase peak concentration of particles. This trend is identical for total concentration of particles. It can also be observed from figure 10 that the distribution width of particulate size increases with increasing intake air temperature. For intake air temperature of 150, 160, 170 and 180 °C at constant fuel quantity (25mg/ Stroke) of methanol, peak particle concentrations appear around mobility sizes of 32, 34, 36, 37 nm with peak concentrations of 1.54×10^8, 1.79×10^8, 1.81×10^8 and 1.52×10^8 particles/cm^3 respectively. Figure 10 suggests that on increasing the intake air temperature, the peak of highest particle concentration shifts towards higher mobility diameters.

SURFACE AREA AND SIZE DISTRIBUTION OF EXHAUST PARTICULATES

The surface area vs. size distribution is very important from toxicology point of view. Higher the surface area, higher will be possibility of surface adsorption of the polycyclic aromatic hydrocarbons (PAHs) and thus higher will be the toxic potential [26]. Smaller particles tend to have significantly higher surface area for the same particle mass compared to larger particle, offering larger surface area for condensation of toxic VOC's and PAH's. Therefore, smaller particles tend to become more hazardous for human health compared to larger particles [17]. The surface area distribution is calculated by the EEPS software using equation $s = \pi D_p^2 n$; D_p is particle mobility diameter and n is number weighted concentration per channel [28]. More details regarding the measurement of number concentration and statistical calculations used are documented in equipment manual [28]. Figure 11 shows some interesting results when the distribution for particle surface area per unit volume of exhaust gases is plotted against the particle size for tests conducted at different fuel quantity injected for a constant intake air temperature condition. As the fueling increases, not only the total area under the particle surface area curve increases but also, the peak shifts towards right, indicating that larger particles start dominating with increase in fuel quantity injected. This trend is opposite of the conventional spark ignition study, where on increasing the engine load, lower particle size contribution is observed to have higher surface area [26]. It is observed the SOI of 70 CAD (IVO injection) and 210 CAD (IVC injection) have higher surface area as compared to other injection timings. This trend is different from the particle number distribution trend due to the fact that surface are distribution dependent on both particle size and number in unit volume of exhaust gas. It can be noticed from the figure 11 that for lower surface area distribution, it is better to have SOI in the IVC condition after 500 CAD. For low fueling rates (21 mg/ Stroke), peak surface area appear around 32 nm with area of 1.12×10^{11} nm^2/cm^3 and for higher fueling rates (25 and 29 mg/ Stroke), peak surface area appears around particle size of 40 and 59 nm with area $6.13\times 10^{11}$and 1.73×10^{12}nm^2/cm^3 respectively. It can be seen that the surface area of particles start dominating in the size range 20-140 nm.

Figure 12 show the variation of surface area distribution with start of injection timing with different intake air temperatures for constant fuel quantity injected (25 mg/ Stroke). It is observed that for each intake air condition, SOI in IVO conditions (70 CAD) have highest peak of surface area and SOI 5 CAD have the lowest peak.SOI in closed valve conditions (500 and 600 CAD) have relatively lower surface area at tested conditions. It is also noticed that peak surface area of particles increases with increase in intake air temperature. It can also be noted from figure 12 that the distribution width of particulate size increases with increasing intake air temperature. For intake air temperature of 150, 160, 170 and 180°C at constant fuel quantity (25mg/ Stroke) of methanol, peak surface area appear around mobility size 40, 54, 56 and 59 nm with peak concentration 6.13×10^{11}, 1.02×10^{12}, 1.15×10^{12} and 1.18×10^{12}nm^2/cm^3 respectively for SOI except 5 CAD. Figure 12 shows that on increasing the intake air temperature, the particles having peak concentration shift towards higher mobility diameters. An order of magnitude higher peak surface area per unit volume

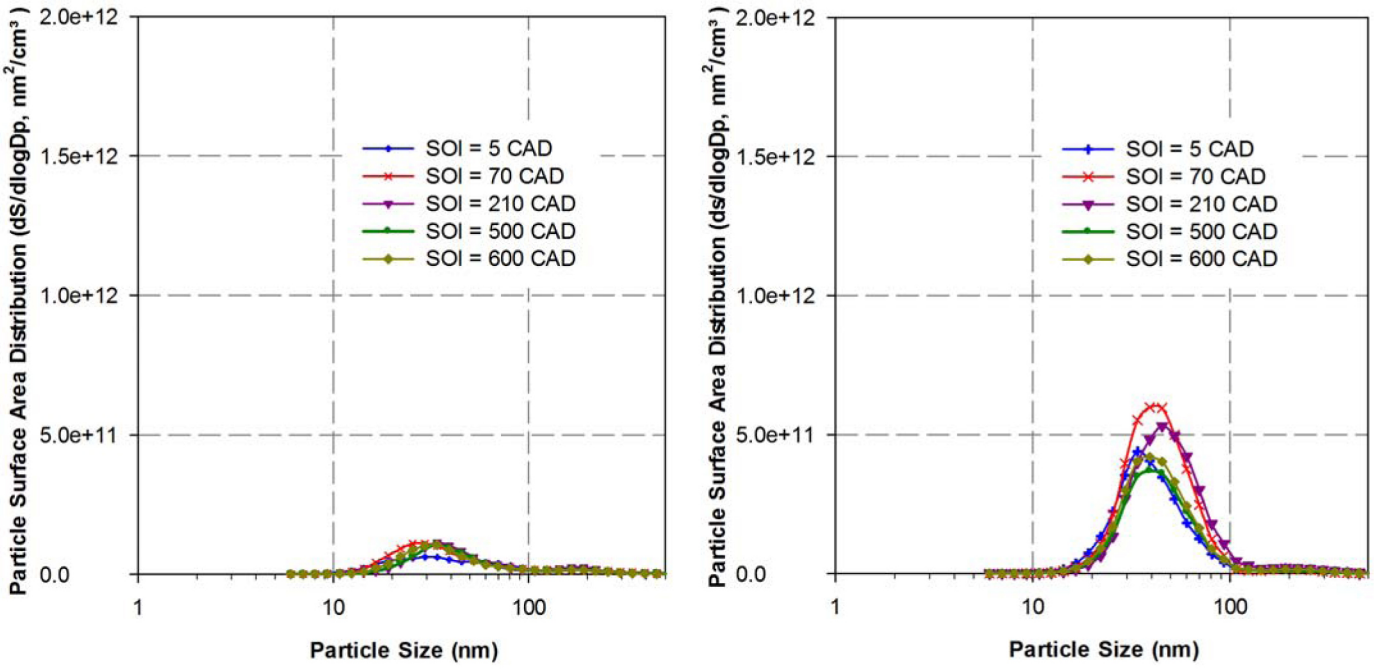

a.21mg/stroke fuel

b. 25 mg/stroke fuel

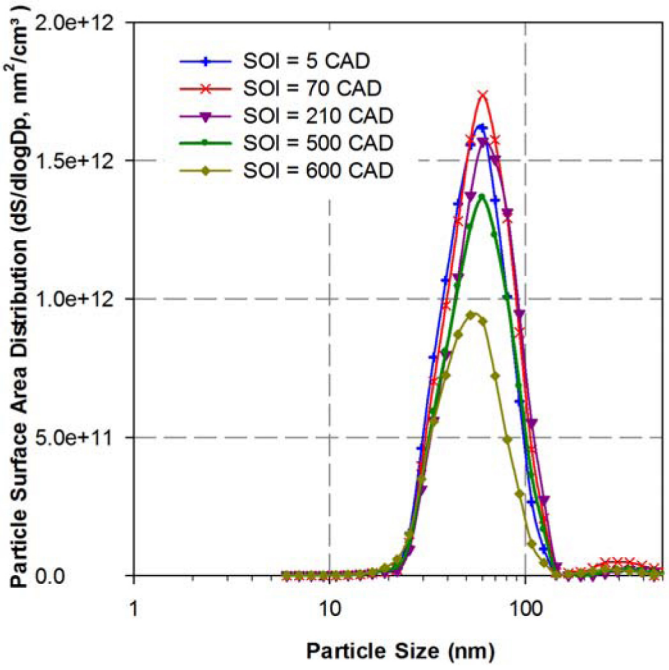

c. 29 mg/stroke fuel

Figure 11. Particle surface area and size distribution at 1500 rpm with varying SOI for different fuel injection quantities.

of exhaust is attained compared to conventional gasoline spark ignition engine [26]. It can be further observed that the higher mobility diameter particles sizes (60 nm) have peaks in surface area distribution curve compared to smaller particle sizes, which show a peak concentration in the number distribution curve.

VOLUME AND SIZE DISTRIBUTION OF EXHAUST PARTICULATES

The volume vs. particle size curve represents the volume/ mass of the particles in that particular size range. Since the mass is higher for larger particles, the possibility of their

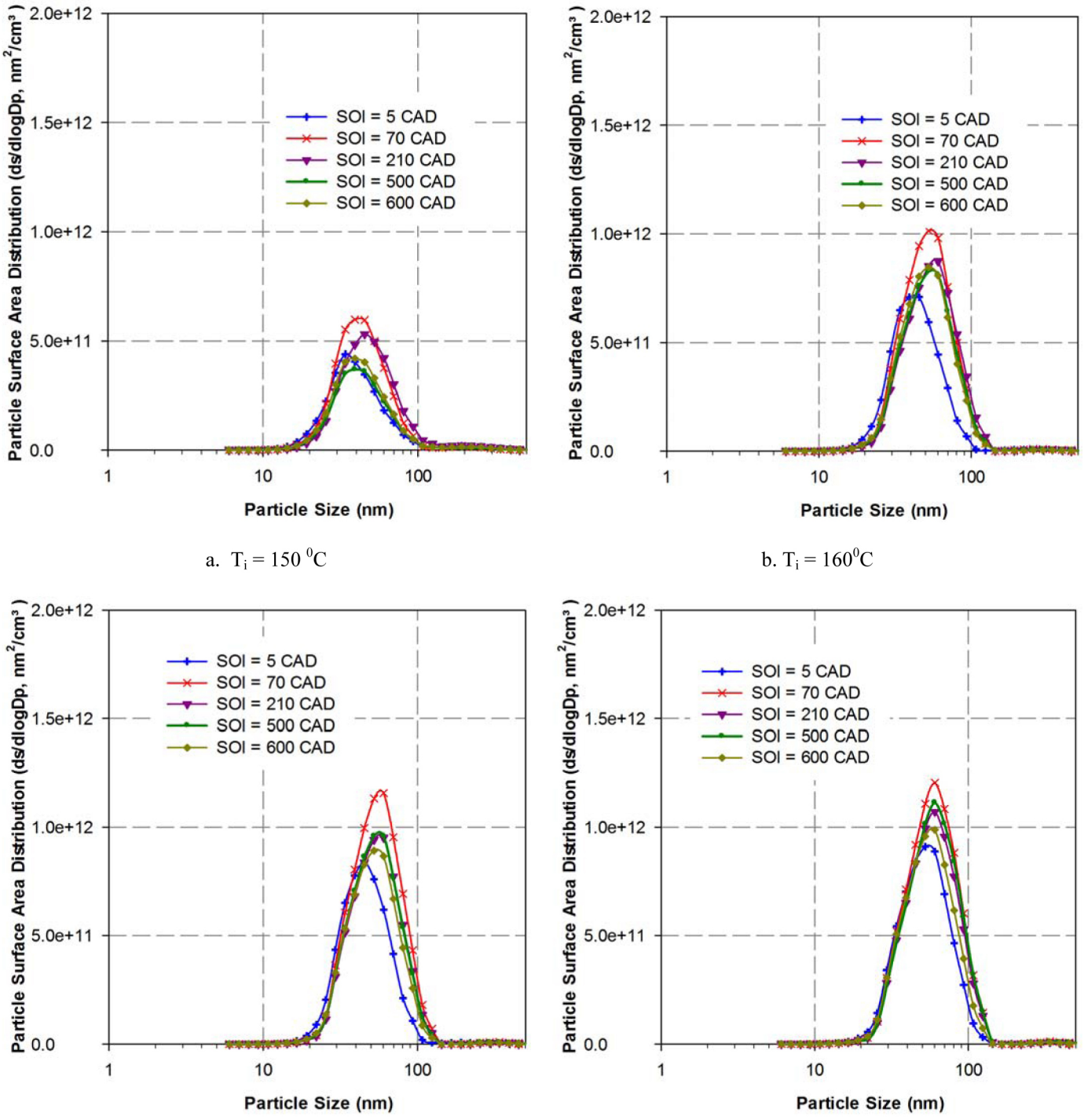

a. $T_i = 150\ ^0C$

b. $T_i = 160^0C$

c. $T_i = 170^0C$

d. $T_i = 180^0C$

Figure 12. Particle surface area and size distribution at 1500 rpm with varying SOI for different inlet air temperature.

settling down will also be higher. The atmospheric retention time for the tiny particles is higher than larger particles for the same reason. The majority of particulate mass is formed during surface growth stage and agglomeration stage thus the residence time during surface growth process has a large influence on the total particulate mass emission. Currently, the cumulative mass of particulate emitted by engines is very important from emission legislation point of view. As of today, global automotive emission regulations rely on compliance of mass emission of particulates and they do not give any weightage to the size and number distribution. This is a skewed way because the heavier particles are less harmful and they do contribute to the mass. On the other hand, large number of tiny particles will be more harmful

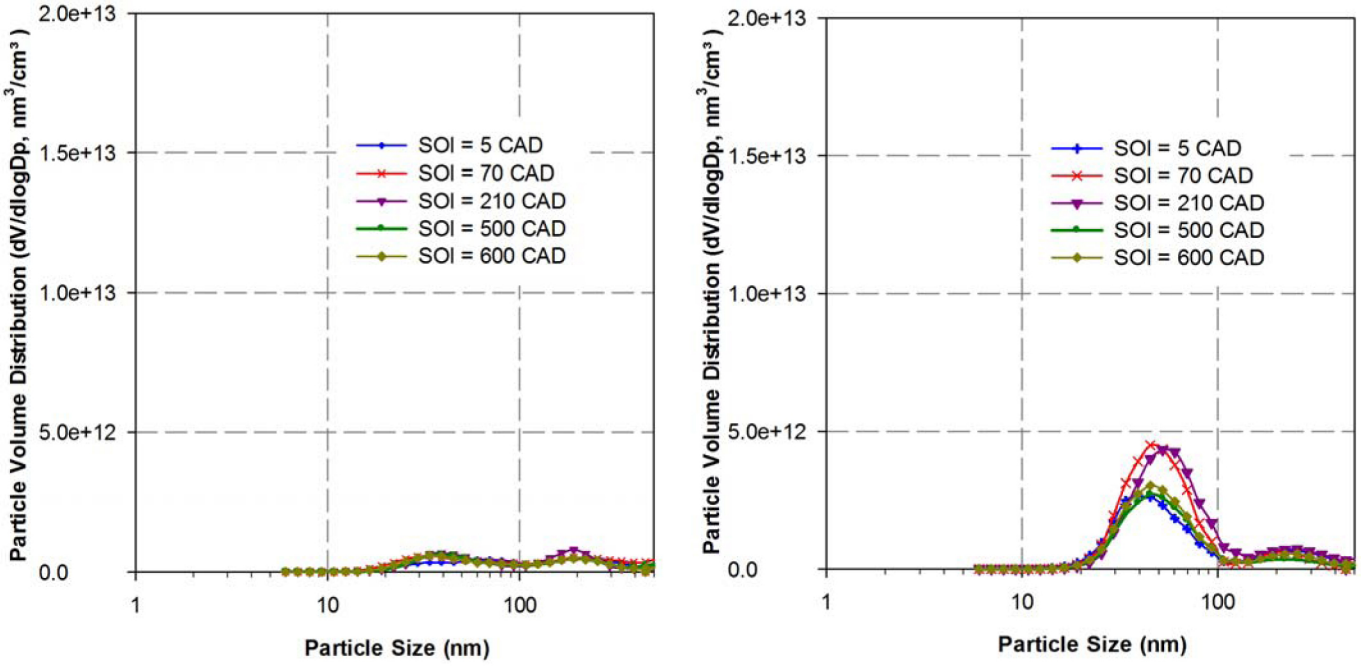

a.21mg/stroke fuel

b. 25 mg/stroke fuel

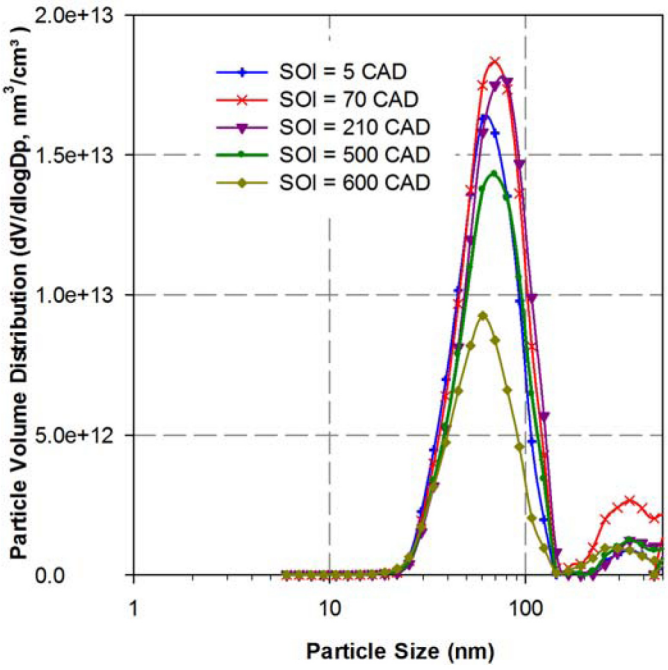

c. 29 mg/stroke fuel

Figure 13. Particle volume and size distribution at 1500 rpm for varying SOI for different fuel injection quantities.

however they won't constitute much mass. Therefore the mass distribution of the particulate becomes important for future emission legislations. With increasing awareness about the harmful effects on human health of nano-particles, law makers will be forced to take cognigence of particulate size, surface area, and mass distributions in future emission norms [17]. The volume distribution is calculated by the EEPS software using equation $v = \pi D_p^3 n/6$; D_p is particle mobility diameter and n is number weighted concentration per channel [28].

Figure 13 shows the conditions when particulate volume distribution is plotted against the particle size for tests conducted at different fuel quantity injected at constant intake air temperature (150°C). The overall volume of the particles will vary proportional to the overall mass of the particulate

assuming that the particle density does not vary with changing size of the exhaust particulate. This is exactly what is seen here also. The particle number distribution is dominating in the lower size range whereas the overall particle volume distribution has prominent peaks in the large particle size range. As the fuel quantity injected increases, total area under the particle volume distribution curve also increases as well as the peak shifts towards right indicating that larger particles dominate this curve. This trend is similar to the trend observed for surface area distribution also. It is observed the SOI of 70 CAD (IVO injection) and 210 CAD (IVC injection) have higher volume as compared to other injection timings, similar to the surface area curve. It can be noticed from figure 13 that for obtaining lower peak for volume distribution, it is desirable to have SOI timing with the IVC injection after 500 CAD. For low fueling (21 mg/ Stroke), peak of volume distribution curve appears for size of 37 nm particles (Volume 6.72×10^{11} nm^3/cm^3) and for higher fueling (25 and 29 mg/ Stroke), peak of volume distribution appears around for particle sizes of 46 and 69 nm with Volumes 4.46×10^{12} and 1.83×10^{13} nm^3/cm^3 respectively. Mobility diameters are larger for peaks of volume density as compared to surface area distribution.

Figure 14 shows the variation of volume distribution with start of injection timing at different intake air temperature for constant fueling (25 mg/Stroke). It is observed that for each intake air condition, SOI in IVO conditions (70 CAD) gives highest peak of volume curve and SOI 5 CAD gives the lowest peak. The trend is very similar to the trend observed in surface area distribution. It can also be seen that peak of volume distribution of particles increases with increase in intake air temperature. It can also be observed from figure14 that the distribution width of particulate size increases with increasing intake air temperature. For intake air temperatures of 150, 160, 170 and 180 °C at constant fueling (25mg/ Stroke) of methanol, peak volume appear around particle mobility size of 47, 60, 61 and 68 nm with peak concentrations 4.53×10^{12}, 9.81×10^{12}, 1.16×10^{13} and $1.27\times10^{13}nm^3/cm^3$ respectively for SOI except 5 CAD. Figure14 shows that on increasing the intake air temperature, the particle size giving peak concentration shifts towards higher mobility diameters. It is also noticed that particles having peak volume distribution have larger sizes (up to 70 nm) as compared to peak surface area (up to 60 nm) and particle number concentration (up to 40 nm).

CONCLUSIONS

Experimental investigations are conducted on a HCCI combustion engine operating at different inlet air temperature and amount of fuel injected by varying SOI timings at engine speed of 1500 rpm using methanol as fuel. EEPS was used to measure size and number distribution of PM. The conclusions of this investigation can be summarized as follows.

• Particulate matter emissions are sensitive to mixture homogeneity and more homogeneity ensures lower PM emissions.

• HC emissions are function of the PFI injection timing for different amount of fuel injected per stroke. Unburned HC emissions during closed valve injection are almost constant and independent of the fuel injection timing. The HC emissions are found to be higher when injection is done with open valves.

• Injection timings during closed intake valve improved the charge homogeneity and reduced the PM emissions. It is observed that total particle number concentration is highest for IVO injection timing of fuel for all tested conditions. For each fueling condition, SOI in IVO conditions (5 and 70 CAD) have higher peak of number concentration as compared to SOI in IVC conditions.

• On increasing the fuel quantity injected and inlet air temperature, the particles having peak number concentration shift towards higher mobility diameter. The particle size around which peak number concentration of particles is measured is less than 40 nm for all test conditions. Particle distribution width of particulate size increases with increasing fueling and inlet air temperature to combustion chamber and for all the test conditions, the particle sizes having significant number of emitted particles are in the range of 10- 150 nm.

• On increasing fueling, total area under the particle surface area curve increases and the peak shifts towards right, indicating that larger particles dominate with increase in fuelling/load. Similar curve is observed for volume distribution with particle size. For lower surface area/ volume per unit volume of exhaust gas, the best SOI is the IVC injection after 500 CAD.

• This investigation suggests that optimum SOI is IVC injection conditions around 500 CAD.

• In summary, HCCI engines are known for its potential for extremely low mass particulate emission however their contribution in terms of particulates number emission can be significant.

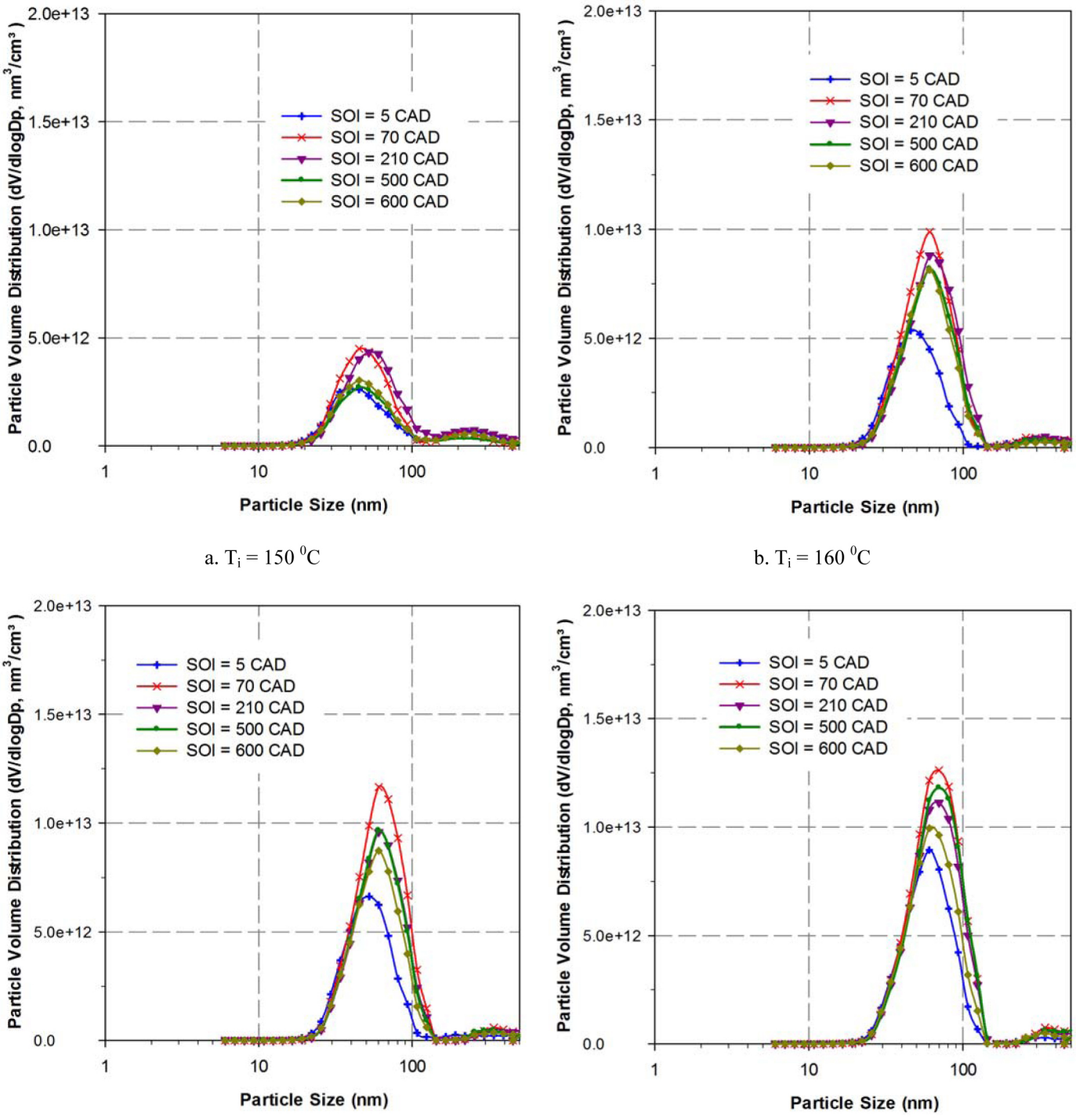

a. $T_i = 150\ ^0C$

b. $T_i = 160\ ^0C$

c. $T_i = 170\ ^0C$

d. $T_i = 180\ ^0C$

Figure 14. Particle volume and size distribution per cm3 at 1500 rpm with varying SOI for different inlet air temperature.

REFERENCES

1. Onishi, S., Hong Jo, S. Shoda, K., Do Jo, P. et al., "Active Termo-Atmosphere Combustion (ATAC) - A New Combustion Process for Internal Combustion Engines," SAE Technical Paper 790501, 1979, doi: 10.4271/790501.

2. Noguchi, M., Tanaka, Y., Tanaka, T., and Takeuchi, Y., "A Study on Gasoline Engine Combustion by Observation of Intermediate Reactive Products during Combustion," SAE Technical Paper 790840, 1979, doi: 10.4271/790840.

3. Maurya, R.K., and Agarwal, A.K., "Experimental investigation of the effect of the intake air temperature and mixture quality on the combustion of a methanol and gasoline-fuelled homogeneous charge compression ignition engine", *Proc. IMechE Part D: Journal of Automobile engineering* **223**(11): 1445-1458, 2009, doi: 10.1243/09544070JAUTO1238.

4. Maurya, R.K., and Agarwal, A.K., "Experimental study of combustion and emission characteristics of ethanol fuelled port injected homogeneous charge compression ignition (HCCI) combustion engine", *Applied Energy* **88** (4): 1169-1180, 2011, doi: 10.1016/j.apenergy.2010.09.015.

5. Maurya, R.K., and Agarwal, A.K., "Experimental investigation on the effect of intake air temperature and air-fuel ratio on cycle-to-cycle variation of HCCI combustion and performance parameters", *Applied Energy* **88** (4): 1153-1163, 2011, doi: 10.1016/j.apenergy.2010.09.027.

6. Christensen, M., Johansson, B., and Einewall, P., "Homogeneous Charge Compression Ignition (HCCI) Using Isooctane, Ethanol and Natural Gas - A Comparison with Spark Ignition Operation," SAE Technical Paper 972874, 1997, doi: 10.4271/972874.

7. Christensen, M., Johansson, B., Amnjus, P., and Mauss, F., "Supercharged Homogeneous Charge Compression Ignition," SAE Technical Paper 980787, 1998, doi: 10.4271/980787.

8. Eng, J.A., "Alternative fuels and fuel Additives for HCCI engines", Homogeneous Charge Compression Ignition (HCCI) Engines: Key Research and Development Issue. Edited by Zhao, Frank et.al. USA: SAE International, 2003.

9. Hall, D.E., King, D.J., Morgan, T.B.D., Baverstock, S.J. et al., "A Review of Recent Literature Investigating the Measurement of Automotive Particulate; The Relationship with Environmental Aerosol, Air Quality and Health Effects," SAE Technical Paper 982602, 1998, doi: 10.4271/982602.

10. Scherrer, H.C., Kittelson, D.B., and Dolan, D.F., "Light Absorption Measurements of Diesel Particulate Matter," SAE Technical Paper 810181, 1981, doi: 10.4271/810181.

11. Kittleson, D.B., "Engines and nano-particles: a review", *Journal of Aerosol Science* **29** (5-6):575-88, 1998, doi: 10.1016/S0021-8502(97)10037-4.

12. Epping, K., Aceves, S., Bechtold, R., and Dec, J., "The Potential of HCCI Combustion for High Efficiency and Low Emissions," SAE Technical Paper 2002-01-1923, 2002, doi: 10.4271/2002-01-1923.

13. Kaiser, E. W., Yang, J., Culp, T., and Maricq, M. M., "Homogeneous charge compression ignition engine-out emissions-does flame propagation occur in homogeneous charge compression ignition?", International *Journal of Engine Research* **3**(4):185-195, 2002, doi: 10.1243/146808702762230897.

14. Price, P., Stone, R., Misztal, J., Xu, H. et al., "Particulate Emissions from a Gasoline Homogeneous Charge Compression Ignition Engine," SAE Technical Paper 2007-01-0209, 2007, doi:10.4271/2007-01-0209.

15. Misztal, J., Xu, H., Tsolakis, A., Wyszynski, M. L., Constandinides, G., Price, P., and Qiao, J., "Influence of inlet air temperature on gasoline HCCI particulate emissions", *Combustion Science and Technology* **181**(5):695-709, 2009, doi: 10.1080/00102200902851610.

16. Misztal, J., Xu, H. M., Wyszynski, M. L., Price, P., Stone, R., and Qiao, J., "Effect of injection timing on gasoline homogeneous charge compression ignition particulate emissions", *International Journal of EngineResearch* **10**(6):419-430, 2009, doi: 10.1243/14680874JER04409.

17. Maurya, R.K., Srivastava, D.K., and Agarwal, A.K., "Experimental Investigations of Particulate Emitted by an Alcohol-Fuelled HCCI/CAI Combustion Engine", *International Energy Journal* **12** (1), 2011.

18. Maurya, R.K. and Agarwal, A.K., "Experimental Investigation of Cycle-by-Cycle Variations in CAI/HCCI Combustion of Gasoline and Methanol Fuelled Engine," SAE Technical Paper 2009-01-1345, 2009, doi: 10.4271/2009-01-1345.

19. Herold, R. E, Foster, D. E., Ghandhi, J. B., Iverson, R. J., Eng, J. A., and Najt, P. M., "Fuel unmixedness effects in a gasoline homogeneous charge compression ignition engine", *International Journal of Engine Research* **8** (3): 241-257, 2007, doi: 10.1243/14680874JER00307.

20. Lang, K.R. and Cheng, W.K., "Effects of Fuel Injection Strategy on HC Emissions in a Port-Fuel-Injection Engine During Fast Idle," SAE Technical Paper 2006-01-3400, 2006, doi:10.4271/2006-01-3400.

21. Wang, T, Peng, Z, Liu, S-L, Xiao, H-D, and Zhao, H., "Optimization of stratification combustion in a spark ignition engine by double-pulse port fuel injection", *Proc. IMechE Part D:Journal of Automobile Engineering* **221**(7): 845-857, 2007, doi: 10.1243/09544070JAUTO376.

22. Robert Bosch GmbH, "Gasoline Engine Management" 3rd Edition, Wiley USA, 2006, ISBN: 978-0-470-05757-5.

23. Maurya, R.K., and Agarwal, A.K., "Statistical Analysis of the Cyclic Variation of Heat Release Parameters in HCCI Combustion of Methanol and Gasoline," Applied Energy 89 (1): 228-236, 2012, doi: 10.1016/j.apenergy.2011.07.002.

24. Dec, J.E. and Sjöberg, M., "Isolating the Effects of Fuel Chemistry on Combustion Phasing in an HCCI Engine and the Potential of Fuel Stratification for Ignition Control," SAE Technical Paper 2004-01-0557, 2004, doi: 10.4271/2004-01-0557.

25. Alkidas, A.C. and Drews, R.J., "Effects of Mixture Preparation on HC Emissions of a S.I. Engine Operating Under Steady-State Cold Conditions," SAE Technical Paper 961958, 1996, doi: 10.4271/961958.

26. Gupta, T., Kothari, A., Srivastava, D.K., and Agarwal, A.K., "Measurement of number and size distribution of particles emitted from a mid-sized transportation multipoint port fuel injection gasoline engine", *Fuel***89**(9): 2230-2233, 2010, doi: 10.1016/j.fuel.2009.12.014.

27. Franklin, L., "Effects of homogeneous charge compression ignition (HCCI) control strategies on particulate emissions of ethanol fuel" PhD Thesis, University of Minnesota, December 2010.

28. Engine Exhaust Particle Sizer™ Spectrometer Model 3090, Operation and Service Manual, TSI, USA, March 2009.

DEFINITIONS/ABBREVIATIONS

BDC
bottom dead center

CAD
crank angle degree

CA50
crank angle position corresponding to 50% burn fraction

CI
compression ignition

DISI
direct injection spark ignition

EOI
end of injection

EEPS
engine exhaust particle sizer

HCCI
homogeneous charge compression ignition

IMEP
indicated mean effective pressure

IVC
intake valve closed

IVO
intake valve open

NVO
negative valve overlap

PFI
port fuel injection

PM
particulate matter

SMPS
scanning mobility particle sizer

SOI
start of injection

TDC
top dead center

T_i
inlet air temperature

About the authors

Rakesh Kumar Maurya (rakesh@iitk.ac.in) is doctoral research student under the supervision of Dr. A. K. Agarwal. He has completed his dual degree M.Tech./B.Tech. program in mechanical engineering from IIT Kanpur under the supervision of Dr A K Agarwal in 2006. His areas of current interest are HCCI Combustion and control, instrumentation, combustion and emission control of IC engine, alternative fuels.

Dr. Avinash Kumar Agarwal (akag@iitk.ac.in) is currently faculty of mechanical engineering at IIT Kanpur since March 2001. His areas of current interest are combustion phenomenon study in IC engines, automotive emission control, biodiesel development and characterization, laser diagnostic techniques, PIV, lubricating oil consumption reduction, lubricating oil tribology, development of micro sensors, and alternative fuels for diesel engines.